CHIN. PHYS. LETT. Vol. 33, No. 10 (2016) 107601

Electron Spin Decoherence of Nitrogen-Vacancy Center Coupled to Multiple Spin Baths *

Jian Xing(邢健)[1], Yan-Chun Chang(常彦春)[1], Ning Wang(王宁)[1],
Gang-Qin Liu(刘刚钦)[1], Xin-Yu Pan(潘新宇)[1,2]**

[1]*Beijing National Laboratory for Condensed Matter Physics, Institute of Physics, Chinese Academy of Sciences, Beijing 100190*
[2]*Collaborative Innovation Center of Quantum Matter, Beijing 100871*

(Received 2 August 2016)

We present the experimental results of nitrogen-vacancy (NV) electron spin decoherence, which are linked to the coexistence of electron spin bath of nitrogen impurity (P1 center) and ^{13}C nuclear spin bath. In previous works, only one dominant decoherence source is studied: P1 electron spin bath for type-Ib diamond; or ^{13}C nuclear spin bath for type-IIa diamond. In general, the thermal fluctuation from both spin baths can be eliminated by the Hahn echo sequence, resulting in a long coherence time (T_2) of about 400 μs. However, in a high-purity type-IIa diamond where ^{13}C nuclear spin bath is the dominant decoherence source, dramatic decreases of NV electron spin T_2 time caused by P1 electron spin bath are observed under certain magnetic field. We further apply the engineered Hahn echo sequence to confirm the decoherence mechanism of multiple spin baths and quantitatively estimate the contribution of P1 electron spin bath. Our results are helpful to understand the NV decoherence mechanisms, which will benefit quantum computing and quantum metrology.

PACS: 76.30.Mi, 76.60.Lz, 76.70.Dx DOI: 10.1088/0256-307X/33/10/107601

The nitrogen-vacancy (NV) center in diamond has drawn much attention in recent years, as a promising candidate for quantum information process, quantum metrology and sensing. It also acts as a good solid-state platform for studying the quantum dynamics of spin systems.[1,2] Due to many unique advantages, ensemble NV centers have been used for hybrid qubits, precise quantum sensing[3–6] and imaging of magnetic field or living cells.[7–9] The increase of NV numbers greatly enhances the coupling strength with other qubit systems, such as superconductor qubit[10–14] and mechanical resonators.[15,16] A large number of NV centers can also improve the signal-to-noise ratio with the enhancement of fluorescence. However, larger NV number is often accompanied by higher concentration of nitrogen impurities, which will reduce the coherence time. Thus it is crucially important to fully exploit the decoherence mechanism of ensemble NV electron spin, especially the contribution from nitrogen electron spin bath.

To investigate the decoherence mechanism of ensemble NV electron spins, many works have been implemented recently. Previous works can be roughly grouped into three classes according to the decoherence sources (Table 1). The first class (lines 1 and 2 in Table 1) is type-Ib diamond or N-doped diamond, which has high nitrogen concentration of about hundred ppm. The extra unbonded electron spins from nitrogen atom (called P1 center) form a fast fluctuation electron spin bath, and dominate the decoherence of NV electron spin in these samples, resulting in a T_2 of only several microseconds.[2,17,18] The second class sample is type-IIa diamond (lines 4–6 in Table 1) which has much lower nitrogen concentration ($<$ 1 ppm). The ^{13}C nuclear spin bath becomes the main source of NV electron spin decoherence and T_2 reaches hundreds of microseconds.[1,17,19] The third class sample (lines 7 and 8 in Table 1) has reduced ^{13}C concentration (0.01%) by isotopical engineering, thus P1 electron spin bath contributes significantly to the decoherence of NV electron spin in these samples.[3,17,18] Bar-Gill *et al.* found that the presence of dense ^{13}C nuclear spin bath can suppress the electronic spin-bath dynamics, which enhances the efficacy of dynamical decoupling pulses on NV electron spin.[18]

In this work we present the direct experimental evidence of both P1 electron and ^{13}C nuclear spin baths contributing to the decoherence of NV electron spin. We measure the coherence time T_2 of NV electron spin under different magnetic fields, and find dramatic decrease related to the resonance of P1 electron spin under certain magnetic field. As shown in Fig. 1(a), with the presence of both ^{13}C nuclear spin bath (green arrows) and P1 electron spin bath (orange arrows), the strong coupling to spin environment results in a very short coherence time of NV electron spin. By applying the Hahn echo sequence, fluctuation of both spin baths can be suppressed, and a much longer coher-

*Supported by the National Basic Research Program of China under Grant Nos 2014CB921402 and 2015CB921103, the Strategic Priority Research Program of the Chinese Academy of Sciences under Grant No XDB07010300, and the National Natural Science Foundation of China under Grant No 11574386.

**Corresponding author. Email: xypan@iphy.ac.cn

© 2016 Chinese Physical Society and IOP Publishing Ltd

ence time is expected (Fig. 1(b)). Furthermore, one can selectively pick up a certain type of spin bath by decoupling other baths, and quantitatively characterize the contribution of a specific bath from the change of T_2, as shown in Fig. 1(c).

Table 1. Comparison of the samples investigated in previous works and in this study.

N (cm^3)	^{13}C	T_2 (μs)	Dominating impurity	Refs.
$\sim 10^{19}$	1.1%	2	^{14}N	Refs. [17,18]
$\sim 5\times10^{18}$	1.1%	5	^{14}N	Ref. [18]
$\leq 10^{17}$	1.1%	380	^{13}C&^{14}N	Our sample
$\sim 10^{16}$	1.1%	300	^{13}C	Ref. [17]
$\sim 5\times10^{15}$	1.1%	282	^{13}C	Ref. [1]
$\sim 10^{15}$	1.1%	630	^{13}C	Refs. [1,19]
$\sim 10^{17}$	0.01%	300	^{14}N	Refs. [17,18]
$\sim 10^{15}$	0.01%	$\sim$500	^{14}N	Ref. [3]

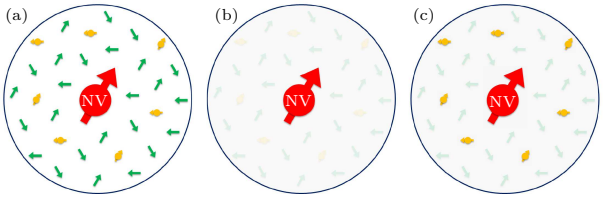

Fig. 1. (Color online) The diagram of the spin baths coexistence. (a) In type-IIa diamond sample, the dominant source of electron spin decoherence is the ^{13}C nuclear spin bath (green arrows). There are also some paramagnetic centers coexisting with the NV center, for example, nitrogen donors with one unpaired electron spin (the P1 centers, orange arrows). (b) Quasistatic noise can be eliminated by the Hahn echo or other dynamic decoupling techniques, and the coherence time T_2 will be prolonged. Here T_2 is derived from the envelop decay of the Hahn echo measurement. (c) When the influence of the quasistatic P1 centers noise remains unchanged during the 'Hahn echo' process, the main source of electron spin decoherence becomes the P1 centers.

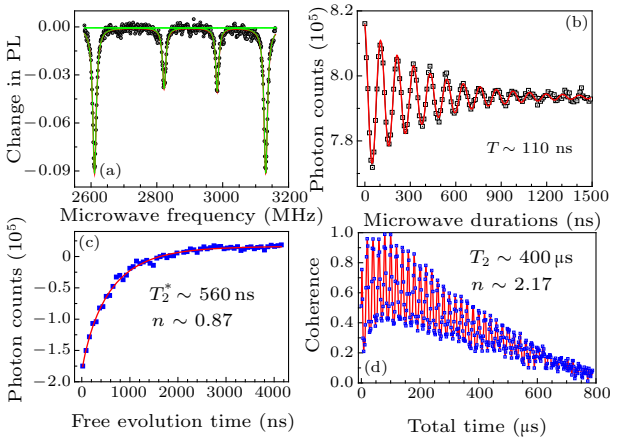

Fig. 2. (Color online) The basic properties of the investigated sample. (a) Typical ODMR spectra of our sample. The magnetic field is along one of the crystallographic axes. The outer two dips of the spectrum are deep, and the numbers of NV centers along these crystallographic axes are larger than those along other axes. (b) The Rabi oscillation of this sample decays quickly. (c) The value of T_2^* of this sample is about 560 ns. (d) The collapses and revivals induced by ^{13}C are shown in the Hahn echo. Here T_2 is about 400 μs.

Our experiment is implemented with a home-built laser scanning confocal microscope system. A high-purity chemical vapor deposition (CVD) single crystal diamond from Element Six (N concentration < 1 ppm) is used. The NV center density of this diamond is $\sim 10^{14}\,\mathrm{cm}^{-3}$ even no ion implantation or annealing treatment is applied. Typical ODMR spectrum of our sample is presented in Fig. 2(a). The Rabi oscillation is shown in Fig. 2(b). Free induction decay (FID) indicates that T_2^* of this sample is about 0.5 μs (see Fig. 2(c)).

To investigate the decoherence behaviors of these NV spins, we apply the Hahn echo sequence with various strengths of external magnetic field. As shown in Fig. 2(d), the coherence time T_2 of this sample under a magnetic field of 200 G is about 400 μs. Collapse and revivals induced by the Larmor precession of the ^{13}C nuclear spin under external magnetic field are observed evidently in the Hahn echo envelope. We note that the coherence of electron spin does not reach zero before it revives again, and this usually happens under a magnetic field of medial strength, as predicted in Ref. [2]. These results indicate that the Overhauser field fluctuation of the ^{13}C spin bath is the main source of decoherence for NV spins in this sample.

The dynamics of spin bath can be controlled by tuning the strength of the external magnetic field, resulting in different decoherence behaviors of NV electron spin. As shown in Fig. 3(a), we find that the envelope of the Hahn echo changes drastically at some specific magnetic fields around 500 G. The coherence time T_2 decreases from 400 μs to 140 μs, indicating a significant difference in ambient spin environment. Previous works have studied effects of fluorescence intensity,[22,23] ^{14}N polarization,[24] Rabi oscillation decay[23] and T_1 decay,[25] at the similar magnetic field. Most of these effects are caused by spin exchange between NV center and P1 center spins.[20,21] We attribute the dramatic decrease of T_2 to the resonance between P1 electron spin bath and NV electron spin under those magnetic fields.

The Hamiltonians of the NV center and P1 spins read

$$H_{\mathrm{NV}} = D(S_z^{\mathrm{NV}})^2 + \gamma_{\mathrm{NV}} B S_z^{\mathrm{NV}}, \quad (1)$$

$$H_{\mathrm{P1}} = \gamma_{\mathrm{N}} B S_z^{\mathrm{N}} + A\boldsymbol{S}^{\mathrm{N}} \cdot \boldsymbol{I}^{\mathrm{N}}, \quad (2)$$

where $\gamma_{\rm NV} \approx \gamma_{\rm N}$ is the gyromagnetic ratio for the NV center and P1 center spins, $S^{\rm NV}$ and $\boldsymbol{S}^{\rm N}$ are the electron spin operators, and $\boldsymbol{I}^{\rm N}$ is the nuclear spin operator of the N atom.[22] The energy levels of the NV centers and P1 center spins are shown in Fig. 3(b) as a function of magnetic field B. The energy splitting between $m_{\rm s} = 0$ and $m_{\rm s} = -1$ energy levels of NV centers matches with the splitting between $m_{\rm s} = +1/2$ and $m_{\rm s} = -1/2$ energy levels of P1 center spins under specified magnetic fields. Due to the hyperfine structure of P1 center spins (^{14}N nuclear spin), there are three resonances of magnetic field values for each P1 center. Furthermore, the relative orientation between NV and P1 centers has two sets, one is parallel to each other and the other has an angle of 109.5° between them. Each set has 3 resonant magnetic field, and they share the same value when ^{14}N nuclear spin is at $m_{\rm s} = 0$ substate, thus there are 5 resonant magnetic values in total.

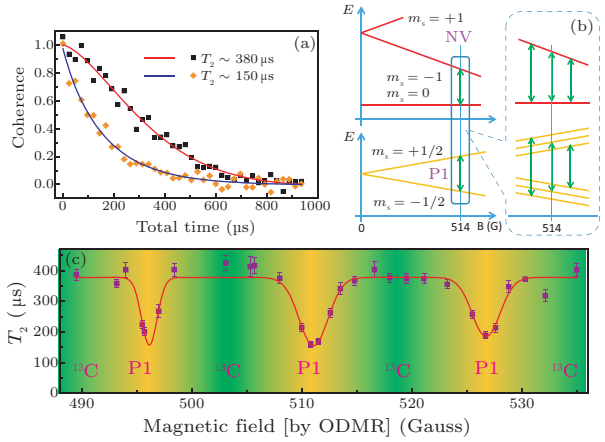

Fig. 3. (Color online) The coexistence of two types of spin bath. (a) The Hahn Echo at different magnetic fields. At most magnetic fields, T_2 is about 400 μs, while at some special magnetic fields, T_2 drops to about 150 μs. (b) Energy levels of the NV center and P1 centers as a function of magnetic field B. Three different energy resonances for NV center and P1 centers are shown in the inset as the hyperfine splitting of the P1 centers into triplets. (c) The value of T_2 derived from the Hahn echo decreases rapidly when the magnetic field is set to some special resonant values.

Figure 3(c) summarizes the dependence of T_2 as a function of the external magnetic field strength. Here T_2 decreases rapidly under resonant magnetic fields: 499 G, 514 G and 529 G, which coincide with the resonant values as shown in Fig. 3(b). We note that there are two less obvious dips (the second data point from left and right of this figure), which just match the resonant field of $m_{\rm I} = \pm 1$ substate of the parallel P1 centers. As $\gamma_{\rm NV} \approx \gamma_{\rm N}$, both P1 spin and NV electron spin will be flipped by the same microwave π pulse under resonant magnetic fields. The interaction between P1 electron spin and NV electron spin will survive during the Hahn echo sequence, resulting in short T_2.

To further confirm the co-existence of two decoherence sources in this sample, we design and implement an experiment with the engineered Hahn echo sequence. As shown in Fig. 4(a), an additional π pulse is added to selectively flip P1 electron spins while the standard echo sequence is applied to the NV electron spin. We fix the magnetic field at some off-resonant value. The modified Hahn echo is carried out to measure the coherence time T_2 with various frequencies of the additional π pulse. The T_2 time as a function of the additional π pulse frequency is plotted in Fig. 4(b). Here T_2 time decreases drastically when the frequency of the additional π pulse is resonant with energy splitting of P1 electron spins. The positions of the 5 resonant dips in Fig. 4(b) are determined by the angle between the Jahn–Teller axis of P1 center and NV quantization axis, as well as the hyperfine interaction with ^{14}N nuclear spins ($S = 1$).[26]

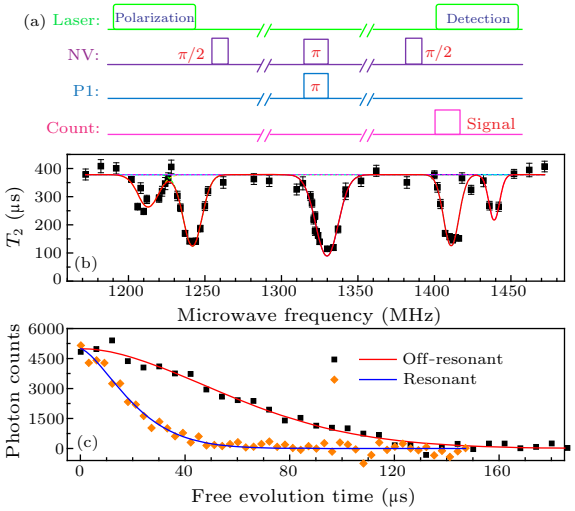

Fig. 4. (Color online) The verification of the spin bath coexistence. (a) The experimental scheme to verify the coexistence of two spin baths. A π pulse for P1 centers is added simultaneously along with the π pulse of NV centers in the Hahn echo. (b) The T_2 time derived from the Hahn echo as a function of the additional π pulse frequency. Five dips are observed when the microwave frequency is resonant with P1 centers. (c) The Hahn echo envelopes of the investigated single NV electron spin, when the P1 centers and NV center are resonant and off-resonant.

The modified Hahn echo is similar to the spin echo double resonance (SEDOR) scheme,[26] and we can calculate the interaction strength $b_{\rm P1}$ between the NV spin and the P1 center spins. The interaction strength $b_{\rm P1}$ derived from the modulated Hahn echo is about $0.024\,\mu s^{-1}$ via $1/T_2' = b_{\rm P1}/\sqrt{2}$, where T_2' is the NV electron spin coherence time with the engineered Hahn echo sequence under resonant conditions (dip values in Fig. 4(b)). The total interaction strength of the whole environment $b_{\rm total}$ is about $2.52\,\mu s^{-1}$ derived from the FID via $1/T_2^* = b_{\rm total}/\sqrt{2}$.[26] Comparing the values of $b_{\rm P1}$ and $b_{\rm total}$, we can conclude that the influence of the P1 center spins is only one percent of the whole environment. The ratio of interaction strength is determined by the ratio of P1 and ^{13}C concentrations.

The N concentration of this sample is about 0.1 ppm. The ^{13}C concentration of this sample is 1.1%. Thus the concentration ratio between ^{13}C and N atoms is of the order of 10^5. Since the nuclear spin gyromagnetic ratio is 3 orders of magnitudes smaller than that of electrons, the effective coupling strength from nuclear spin is 2 orders stronger than that of electrons, which is in agreement with the calculated ratio of interaction strength from the Hahn echo measurement. By measuring the interaction strength, one might be able to optimize the nitrogen concentration more precisely and to prepare a sample with high density NV center and long coherence time, which will benefit all the applications of ensemble NV centers.

Similar results are observed on a single NV center with a T_2^* of 1.6 μs. Collapse and revival with an envelop decay time of about 100 μs are observed in its Hahn echo signal, indicating that ^{13}C nuclear spin bath is the dominant decoherence source of this sample. Figure 4(c) shows the Hahn echo envelopes of the investigated single NV electron spin under resonant and off-resonant magnetic field. When the P1 centers and NV center are off-resonant, the coherence time T_2 extracted from the Hahn echo signal is about 97 μs. However, under the resonant magnetic field of 514 G, T_2 of the same NV center spin drops to 47 μs. Thus we obtain that P1 center spin bath also contributes significantly to the decoherence time of single NV electron spin in high purity diamond.

The observed coexistence of P1 electron spin and ^{13}C nuclear spin gives a new view on understanding the decoherence mechanics of the NV system. Though the concentration of P1 centers is very low, its influence can be significant when the ^{13}C nuclear spin bath is decoupled by the Hahn echo or other dynamical decoupling techniques.

Our results represent a more generalized and elemental demonstration that multiple spin baths, even with very different spin dynamics, can contribute to the decoherence of the same central spin. This model is closely related to the two most attractive applications of NV centers: quantum computing and weak magnetic field sensing. To meet the challenge in scaling up qubit numbers for quantum computing, highly feasible protocols include coupling NV spins to superconductor, mechanical resonators or photon qubits, and multiple decoherence sources is a fundamental problem in those hybrid quantum systems. Moreover, the spin bath from the unbounded atoms on diamond surface is an ever present obstacle in weak magnetic field sensing.[27–30] All these applications require a decoherence model of multiple spin baths, and our results gives a simple and easy start.

In summary, we have presented an experimental study of NV electron spin decoherence in type-IIa diamond. The long coherence time T_2, evident collapse and revivals of this sample, indicate that the Overhauser field fluctuation of the ^{13}C spin bath contributes mainly to the decoherence of NV electron spins. Under the resonant condition the Hahn echo pulses only suppress the ^{13}C spin bath fluctuation. The surviving interaction from P1 electron spin bath, even only one percent of the whole environment in effective strength, causes dramatic decreases of NV electron spin coherence time T_2. This phenomenon can be controlled by the magnetic field or additional microwave pulse. The similar phenomenon is observed in a single NV center of type-IIa diamond from the Sumicrystal company. These results show that the influence of P1 center spins cannot be ignored even in high purity diamond sample. The investigation of this phenomenon helps us to obtain a further understanding of the decoherence mechanisms of the NV system, which is useful for applications of NV centers, for example, hybrid qubit coupling NV centers with superconductor qubit and detection of weak magnetic fields.

References

[1] Stanwix P L et al 2010 *Phys. Rev.* B **82** 201201
[2] Zhao N, Ho S W and Liu R B 2012 *Phys. Rev.* B **85** 115303
[3] Bar-Gill N, Pham L M, Jarmola A, Budker D and Walsworth R L 2013 *Nat. Commun.* **4** 1743
[4] Steinert S et al 2013 *Nat. Commun.* **4** 1607
[5] Zhao N, Hu J L, Ho S W, Wan J T K and Liu R B 2011 *Nat. Nanotechnol.* **6** 242
[6] Zhao N et al 2012 *Nat. Nanotechnol.* **7** 657
[7] Le Sage D et al 2013 *Nature* **496** 486
[8] Schirhagl R, Chang K, Loretz M and Degen C L 2014 *Annu. Rev. Phys. Chem.* **65** 83
[9] McGuinness L P et al 2011 *Nat. Nanotechnol.* **6** 358
[10] Kubo Y et al 2010 *Phys. Rev. Lett.* **105** 140502
[11] Kubo Y et al 2011 *Phys. Rev. Lett.* **107** 220501
[12] Zhu X et al 2011 *Nature* **478** 221
[13] Saito S et al 2013 *Phys. Rev. Lett.* **111** 107008
[14] Marcos D et al 2010 *Phys. Rev. Lett.* **105** 210501
[15] MacQuarrie E R, Gosavi T A, Jungwirth N R, Bhave S A and Fuchs G D 2013 *Phys. Rev. Lett.* **111** 227602
[16] Bennett S D et al 2013 *Phys. Rev. Lett.* **110** 156402
[17] Pham L M et al 2012 *Phys. Rev.* B **86** 045214
[18] Bar-Gill N et al 2012 *Nat. Commun.* **3** 858
[19] Pham L M et al 2011 *New J. Phys.* **13** 045021
[20] Armstrong S, Rogers L J, McMurtrie R L and Manson N B 2010 *Phys. Procedia* **3** 1569
[21] Hanson R, Dobrovitski V V, Feiguin A E, Gywat O and Awschalom D D 2008 *Science* **320** 352
[22] Hanson R, Mendoza F M, Epstein R J and Awschalom D D 2006 *Phys. Rev. Lett.* **97** 087601
[23] Hanson R, Gywat O and Awschalom D D 2006 *Phys. Rev.* B **74** 161203
[24] Fischer R, Jarmola A, Kehayias P and Budker D 2013 *Phys. Rev.* B **87** 125207
[25] Jarmola A, Acosta V M, Jensen K, Chemerisov S and Budker D 2012 *Phys. Rev. Lett.* **108** 197601
[26] de Lange G et al 2012 *Sci. Rep.* **2** 382
[27] Shi F Z et al 2015 *Science* **347** 1135
[28] Arai K et al 2015 *Nat. Nanotechnol.* **10** 859
[29] DeVience S J et al 2015 *Nat. Nanotechnol.* **10** 129
[30] Trifunovic L et al 2015 *Nat. Nanotechnol.* **10** 541